Dissolution of a polyelectrolyte-macroion complex by addition of salt

Marie Skepö* and Per Linse
Physical Chemistry 1, Center for Chemistry and Chemical Engineering, Lund University, P.O. Box 124, S-221 00 Lund, Sweden
(Received 31 January 2002; published 27 November 2002)

The dissolution of complexes formed by a linear polyelectrolyte and oppositely charged macroions by addition of salt has been examined by employing a simple model with focus on the electrostatic interactions and solved by Monte Carlo simulations. In the absence of salt an overcharged complex appears. Upon addition of salt, the number of complexed macroions is continuously decreasing, the effect being similar for flexible and stiff polyelectrolytes. Regarding the flexible polyelectrolyte, the number of polyelectrolyte-macroion contacts is reduced, whereas it remains nearly constant for the stiff polyelectrolyte as the salt content is increased. A screened Coulomb potential of the Debye-Hückel type, in which the small ions are only indirectly described, displays a good representation of the system.

DOI: 10.1103/PhysRevE.66.051807 PACS number(s): 61.25.Hq

I. INTRODUCTION

Polyelectrolytes are polymers bearing ionizable groups, which, in polar solvents, can dissociate into charged polymers and small counterions. The long-ranged character of the electrostatic interactions gives polyelectrolytes specific properties [1]. In aqueous solutions, polyelectrolytes may interact strongly with other macroions [2–5], and in particular they tend to associate with objects of opposite charge and form complexes. Such objects can be another polyelectrolyte, a colloidal particle, a protein, a micelle, or a vesicle formed by surfactants.

One common phenomenon in colloidal science is coacervation, i.e., an aqueous solution of macromolecules of opposite charge separates into two immiscible liquid phases. The denser phase, which is relatively concentrated in the macromolecules, is referred to as the coacervate and is in equilibrium with another liquid phase poor in the macromolecules [6]. Addition of salt to the phase separated system often leads to the mixed state again. Such observations were made already in the 1950s, when it was discovered that polyelectrolyte-surfactant complexes could be redissolved by the addition of salt. This was later exploited in the purification of polyelectrolytes, e.g., glucosamionglycans from biological tissues [7]. Other groups have reported similar results (see, e.g., Ref. [8]), and recently it was found that coacervation could be both suppressed and enhanced by the addition of salt in surfactant-polyelectrolyte systems [8–10]. Finally, a biological example is the association of DNA with oppositely charged octamers of histone proteins to form a nucleosome bead. At physiological salt concentrations DNA is tightly wrapped around the histone, whereas at much larger salt concentration DNA is released from the complex [11].

It is thus established that the tendency of forming complexes and the strength of complexes can be modulated by addition of low molecular salt. When a finite concentration of salt is present in the solution, the Coulomb interaction between the remaining charged species becomes effectively screened and the effective potential will decay exponentially instead of algebraically with distance. Thus, when adding salt to a system, the interaction can be tuned from being long ranged to short ranged. Several theories describing the complexation between polyelectrolytes and macroion have recently been proposed [12–15]. Netz and Joanny [12] have presented a theory for the 1:1 complex, i.e., one polyelectrolyte and one macroion, and Kunze and Netz [13] have applied that on the DNA-histone complexation, whereas Nguyen and Shklovskii [14] and Schiessel, Bruinsma, and Gelbart[15] have considered the complexation between one polyelectrolyte and several macroions. In these approaches, the effects of simple salt were also included.

In our previous contributions [16,17], we have presented results from Monte Carlo simulations involving polyelectrolytes complexing oppositely charged macroions. The effects of macroion charge, polyelectrolyte charge, length, and stiffness at different number of macroions on the complexation were investigated. At a stoichiometric excess of macroions, the polyelectrolyte-macroion complex became overcharged by the macroion charges. Flexible polyelectrolytes became overcharged by $\approx$50%, whereas stiff polyelectrolytes displayed a larger overcharging, $\approx$75%.

In this paper we examine how an overcharged complex formed by one polyelectrolyte in a solution of excess macroions dissolves upon addition of simple salt using the so-called primitive model, in which the small ions enter explicitly. Both flexible and stiff polyelectrolytes are considered. As the salt concentration was increased, a smooth transition from an overcharged polyelectrolyte-macroion complex, to a neutral complex, an undercharged complex, and finally a noncomplexed polyelectrolyte appeared. Moreover, a simplified screened Coulomb model, where the effect of the small ions enters only indirectly, has been employed. Comparisons have also been made between predictions of the screened Coulomb model and the primitive model to describe polyelectrolyte solutions [18–22] and more complex solutions [23].

Despite the complexity to solve the primitive model, it is still a simple approach with a focus on the electrostatic interactions. Obviously, at high salt concentration where the Coulomb forces are screened, some of its assumptions become less realistic. For example, other forces as the disper-

*Email address: marie.skepo@fkem1.lu.se

sion force becomes important [24,25] and the dielectric approximation as such becomes questionable. Nevertheless, we believe that the prediction of the primitive model should first be addressed before more advanced approaches are taken.

The outline of the paper is as follows. The model and some simulation aspects are given in Sec. II. In Sec. III, the results regarding binding functions, complexation functions, polyelectrolyte extensions, macroion structure, and the two models are presented and discussed. The article ends with conclusions given in Sec. IV.

II. METHOD

A. Model

Aqueous solutions containing one polyelectrolyte and eight macroions have been examined using two different models. The models used are (i) the primitive model and (ii) a simplified one referred to as the screened Coulomb model. In both of them, the polyelectrolyte is described as a chain of charged hard spheres (segments) connected by harmonic bonds and with the intrinsic flexibility of the chain regulated by harmonic angular potentials. The macroions are modeled as large charged hard spheres with a point charge in the center. In the primitive model, all the small ions are also represented as charged hard spheres with point charges in the center, while in the screened Coulomb model there are no explicit small ions; instead the influence of them is preaveraged by employing a screened Coulomb potential. In both models, the solvent enters only through its relative permittivity.

The total potential energy of the system is given by

$$U = U_{\text{nonbond}} + U_{\text{bond}} + U_{\text{angle}}, \tag{1}$$

where the nonbonded energy is assumed pairwise additive according to

$$U_{\text{nonbond}} = \sum_{i<j} u_{ij}. \tag{2}$$

Within the primitive model, the interaction potential u_{ij} for the pair ij, where i and j denote either a polyelectrolyte segment (seg), a macroion (M), a cation, or an anion, is given by

$$u_{ij}(r_{ij}) = \begin{cases} \infty, & r_{ij} < R_i + R_j \\ \dfrac{Z_i Z_j e^2}{4\pi\varepsilon_0\varepsilon_r}\dfrac{1}{r_{ij}}, & r_{ij} \geqslant R_i + R_j \end{cases}, \tag{3}$$

where Z_i is the charge of particle i, R_i is the radius of particle i,e is the elementary charge, ε_0 is the permittivity of vacuum, and ε_r is the relative permittivity of water. In the screened Coulomb model, the summation in Eq. (2) extends only over chain segments and macroions and u_{ij} is given by an extended Debye-Hückel potential,

$$u_{ij}(r_{ij}) = \begin{cases} \infty, & r_{ij} < R_i + R_j \\ \dfrac{Z_i Z_j e^2}{4\pi\varepsilon_0\varepsilon_r}\dfrac{\exp[-\kappa(r_{ij}-(R_i+R_j))]}{(1+\kappa R_i)(1+\kappa R_j)}\dfrac{1}{r_{ij}}, & r_{ij} \geqslant R_i + R_j \end{cases}, \tag{4}$$

where $\kappa = [(e^2/\varepsilon_0\varepsilon_r kT)\Sigma_i Z_i^2 \rho_i]^{1/2}$ denotes the inverse Debye screening length, in which the summation i extends over the small ions only with ρ_i denoting the number density of small ions of type i,k is the Boltzmann constant, and T is the temperature.

In addition to the electrostatic and hard-sphere interactions, the description of the polyelectrolyte includes harmonic bond and angular potentials. The bond potential energy is given by

$$U_{\text{bond}} = \sum_{i=1}^{N_{\text{seg}}-1} \frac{k_{\text{bond}}}{2}(r_{i,i+1} - r_0)^2, \tag{5}$$

where $r_{i,i+1}$ denotes the distance between two connected segments with the equilibrium separation $r_0 = 5$ Å and the force constant $k_{\text{bond}} = 0.4$ N/m and where N_{seg} denotes the number of segments of the polyelectrolyte. The angular potential energy is represented by

$$U_{\text{angle}} = \sum_{i=2}^{N_{\text{seg}}-1} \frac{k_{\text{ang}}}{2}(\alpha_i - \alpha_0)^2, \tag{6}$$

where α_i is the angle formed by the vectors $\mathbf{r}_{i+1} - \mathbf{r}_i$ and $\mathbf{r}_{i-1} - \mathbf{r}_i$ made by three consecutive segments with the equilibrium angle $\alpha_0 = 180°$ and the force constant k_{ang}. In addition to the angular potential, the electrostatic interaction among the segments also contributes to the rigidity of the polyelectrolyte, and this electrostatic contribution is of course affected by other ionic particles present.

We have considered two different chain flexibilities by using the angular force constants $k_{\text{ang}} = 0$ and 328×10^{-24} J/deg^2, respectively. For a single and uncharged chain, these force constants lead to the persistence lengths $l_p = 7$ and 1480 Å, respectively, where the persistence lengths are evaluated by using $\langle \cos(\pi - \alpha) \rangle$ and the root-mean-square segment-segment separation extrapolated to an infinite long chain [26]. Hence, one flexible and one very stiff polyelectrolyte are considered (cf. $l_p \approx 400$ Å for DNA).

The system volume $V = L^3$ with the box length $L = 258$ Å is used throughout. All investigated systems contain one polyelectrolyte and eight macroions. The polyelectrolyte has $N_{\text{seg}} = 40$ segments, each with one elementary charge, $Z_{\text{seg}} = 1$, making the polyelectrolyte charge $Z_p = N_{\text{seg}} Z_{\text{seg}} = 40$. The macroion has a radius of $R_M = 15$ Å and possesses ten negative elementary charges, which could correspond to a micelle formed by a mixture of ionic and nonionic surfactants or a water-soluble globular protein. The macroion number density becomes $\rho_M = 4.7 \times 10^{-7}$ Å^{-3} and the corresponding volume fraction $\phi_M = (4\pi/3) R_M^3 \rho_M = 0.0066$. All the simulations were performed at $T = 298$ K and $\varepsilon_r = 78.4$. Data of the model systems are compiled in Table I.

TABLE I. Data of the model.

Box length	$L=257.92$ Å
Macroion radius	$R_M=15$ Å
Segment radius	$R_{\text{seg}}=2$ Å
Small ion radius	$R_{\text{ion}}=2$ Å
Macroion charge	$Z_M=-10$
Segment charge	$Z_{\text{seg}}=1$
Small ion charge	$Z_{\text{ion}}=\pm 1$
Number of segments	$N_{\text{seg}}=40$
Number of macroions	$N_M=8$
Number of cations	$N_{\text{cation}}=80-$
Number of anions	$N_{\text{anion}}=40-$
Salt concentration	$c_{\text{salt}}=0-300$ mM
Temperature	$T=298$ K
Relative permittivity	$\varepsilon_r=78.4$

Eight different concentrations of added salt in the range $c_{\text{salt}}=0-300$ mM were considered. These concentrations as well as the corresponding screening lengths are given in Table II. Note that at $c_{\text{salt}}=0$ the counterions of the charged particles are present, i.e., 40 counterions of the polyelectrolyte and 80 of the macroions. At the highest salt concentration, the system contains ≈6200 small positive and negative ions.

B. Simulation aspects

The equilibrium properties of the model systems were obtained from canonical Monte Carlo (MC) simulations according to the standard Metropolis algorithm [27]. The particles were enclosed in a cubic box and periodical boundary conditions were applied. The long-ranged Coulomb interactions were handled by using the Ewald summation technique with conducting boundary conditions (see Refs. [16], [17] for further details). The examination of the configurational space was accelerated by using four different types of displacements of the polyelectrolyte: (i) translational displacement of a single charged particle, (ii) pivot rotation of a part of the polyelectrolyte chain, (iii) translation of the entire polyelectrolyte chain, and (iv) slithering move using a biased sampling technique. The probabilities of different trial moves were selected such that to enable single-particle moves ca. 20 times more often than the pivot movements and the translations of the entire chain and 10 times more often than the slithering movements. The particles were initially placed randomly in the simulation box, and after equilibrium, the length of a production run was in general 2×10^5 MC trial moves per particle. Despite the strong polyelectrolyte-macroion complex, it has previously been shown that in the absence of added salt the present protocol produces an ergodic sampling [16,17].

Reported uncertainties of simulated quantities are one standard deviation of the mean as estimated by dividing the simulations into ten sub-batches. All simulations were using the integrated Monte Carlo/molecular dynamics/Brownian dynamics simulation package MOLSIM [28].

TABLE II. Salt concentration (c_{salt}), Debye screening length (κ^{-1}), and averaged number of complexed segments near a complexed macroion (n_{seg}) using the primitive model.

		n_{seg}[a]	
c_{salt} (mM)	κ^{-1} (Å)	Flexible	Stiff
0	39.6	7.6	4.2
10	24.0	7.7	4.3
25	17.2	7.6	4.3
75	10.6	7.1	4.2
100	9.3	7.0	4.1
150	7.6	6.2	4.0
200	6.6	5.7	3.9
300	5.5	5.0	3.8

[a]Largest estimated uncertainty is $\sigma=0.2$.

III. RESULTS AND DISCUSSIONS

Properties of the polyelectrolyte-macroion solution on the basis of the results from the primitive model will be discussed first, and thereafter results obtained from the primitive model and the screened Coulomb model will be compared.

A. Binding function

As mentioned in Sec. I, it is anticipated that the composition of the polyelectrolyte-macroion complex will change when salt is added to the system. Figure 1 displays typical configurations for the salt concentrations $c_{\text{salt}}=0$, 75, and 300 mM for the flexible [panels (a)–(c)] and the stiff [panels (d)–(f)] polyelectrolyte. At $c_{\text{salt}}=0$ the polyelectrolytes complex five to six macroions [panels (a) and (d)] (see also Ref. [17]), at the intermediate c_{salt} the polyelectrolytes complex four macroions [panels (b) and (e)], whereas at the highest c_{salt} considered the complex is nearly fully dissolved [panels (c) and (f)]. Thus, the snapshots show that the compositions of the polyelectrolyte-macroion complexes vary similarly for the two different chain flexibilities when the salt concentration is increased.

The number of complexed macroions N_M^c as a function of salt concentration, also referred to as a binding function, is displayed in Fig. 2. A macroion is considered to be complexed to the polyelectrolyte if the distance between at least one polyelectrolyte segment and the macroion does not exceed 5 Å from their hard-sphere contact separation. The distance criterion is somewhat arbitrary, but the qualitative aspects of the results are not dependent on it.

For both the flexible and the stiff polyelectrolyte, N_M^c decreases continuously as salt is added. Independent of the chain flexibility, at $c_{\text{salt}}\approx 50-60$ mM the binding function displays a smooth crossover from an overcharged complex (the absolute charge of complexed macroions exceeds that of the polyelectrolyte) to an undercharged one. Moreover, at low c_{salt} the stiffer polyelectrolyte possesses a larger number of complexed macroions as compared to the flexible one [consistent with Figs. 1(a) and 1(d)], whereas at c_{salt}

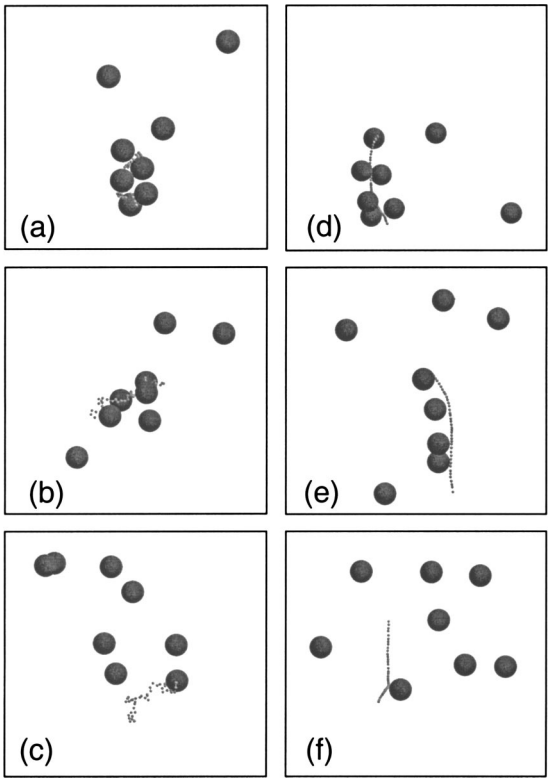

FIG. 1. Typical configurations of systems containing one flexible polyelectrolyte and eight macroions at (a) $c_{\mathrm{salt}}=0$ mM, (b) $c_{\mathrm{salt}}=75$ mM, and (c) $c_{\mathrm{salt}}=300$ mM, and one stiff polyelectrolyte and eight macroions at (d) $c_{\mathrm{salt}}=0$ mM, (e) $c_{\mathrm{salt}}=75$ mM, and (f) $c_{\mathrm{salt}}=300$ mM. The small dots represent polyelectrolyte segments and the spheres macroions. The box length is 258 Å, and the particles are drawn to scale. The small ions are omitted for clarity. Periodic boundary conditions are applied in all three directions to avoid surface artefacts.

>100 mM the flexible polyelectrolyte displays the larger number of complexed macroions. At $c_{\mathrm{salt}}\approx 300$ mM, $N_M^c \approx 0.8$ is obtained, indicating a dominance of a 1:1 complex as displayed in Figs. 1(c) and 1(f). Simulation of the corresponding uncharged systems gave $N_M^c=0.1$; the nonzero value being a pure density effect.

Previously, the binding isotherms for flexible and stiff chains as well as the *difference* in the free energy of complexation macroions to flexible chains and to stiff chains at $c_{\mathrm{salt}}=0$ were examined [17]. It was concluded that a *single* macroion binds stronger to a flexible polyelectrolyte than to a stiff one. As further macroions are complexed to the polyelectrolyte, the difference in the complexation free energy between flexible and stiff chains for the next macroion is reduced and eventually changes in sign. Since, the maximum number of macroion complexed determines at which N_M^c the complexation free energy becomes zero, this sign reversal is consistent with the observation that a larger number of macroions are complexed to the stiff chain as compared to the flexible one at $c_{\mathrm{salt}}=0$ (Fig. 2). As salt is added the electrostatic attraction between the oppositely charged macromolecules are screened, and at $c_{\mathrm{salt}}>100$ mM, at most two macroions are complexed to the polyelectrolyte. The crossing of

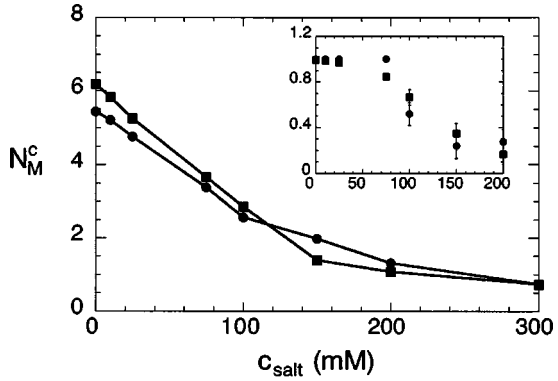

FIG. 2. Number of complexed macroions (N_M^c) vs the salt concentration (c_{salt}) for the flexible (filled circles) and the stiff (filled squares) polyelectrolyte using the primitive model. Largest estimated uncertainty is $\sigma=0.1$. The corresponding dependency for a solution containing one polyelectrolyte and one macroion, at otherwise identical conditions, is shown in the inset.

the two binding functions given in Fig. 2 shows that the higher affinity displayed by the flexible chain to bind one or two macroions at low concentration [17] also prevails at higher salt concentration.

The corresponding binding functions for systems containing one polyelectrolyte and *one* macroion have also been determined. In the absence of salt, such systems form a strong 1:1 complex [16,17]. The inset of Fig. 2 displays that as long as c_{salt} remains below ca. 50 mM, N_M^c is close to 1, whereas N_M^c reduces to 0.5 (50% chance of complexation) at ca. 100 mM and reduces further at higher salt concentration.

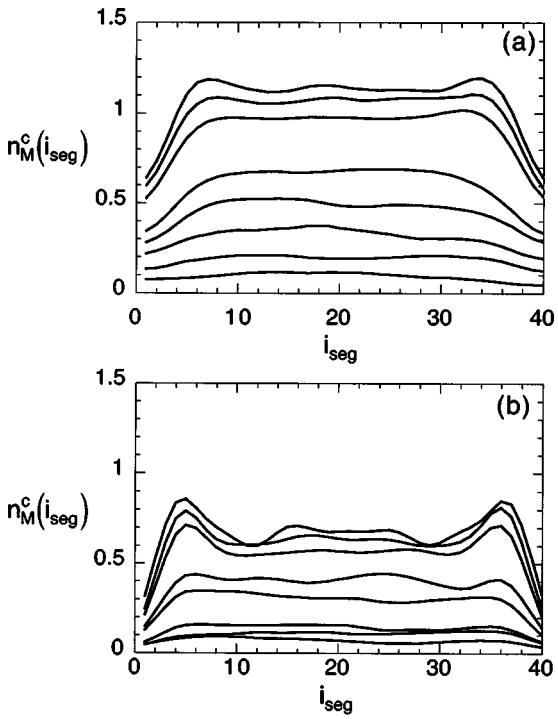

FIG. 3. Total number of complex macroions to a segment $[n_M^c(i_{\mathrm{seg}})]$ vs segment rank (i_{seg}) for (a) the flexible and (b) the stiff polyelectrolyte at $c_{\mathrm{salt}}=0$, 10, 25, 75, 100, 150, 200, and 300 mM (top to bottom) using the primitive model.

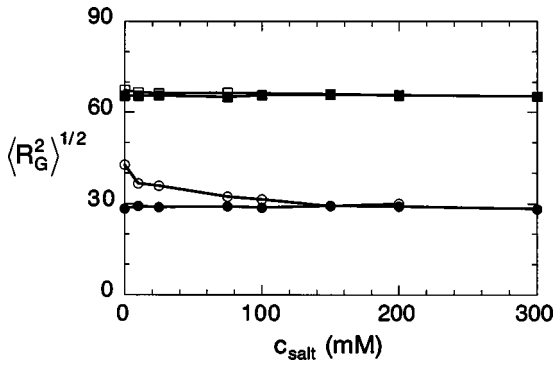

FIG. 4. Radius of gyration of the polyelectrolyte ($\langle R_G^2 \rangle^{1/2}$) vs the salt concentration (c_{salt}) for the flexible polyelectrolyte in the presence (open circles) and absence (filled circles) of macroions and for the stiff polyelectrolyte in the presence (open squares) and absence (filled squares) of macroions using the primitive model. Largest estimated uncertainties are $\sigma = 0.7$ for the flexible and 0.4 for the stiff polyelectrolyte.

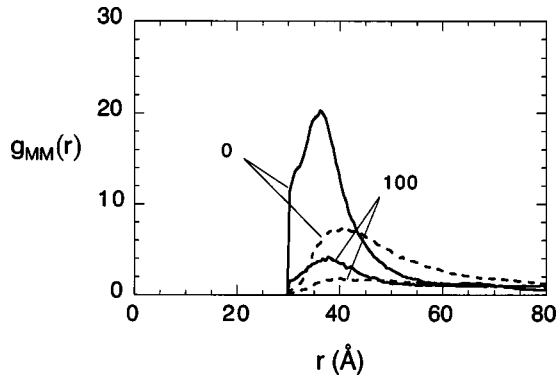

FIG. 5. Macroion-macroion radial distribution function [$g_{MM}(r)$] for the flexible (solid curves) and the stiff (dashed curves) polyelectrolyte at indicated salt concentrations in mM using the primitive model.

B. Complexation function

The nature of the polyelectrolyte-macroion complex has also been examined by considering the complexation function $n_M^c(i_{seg})$, which denotes the average number of complexed macroions to segment i_{seg} of the polyelectrolyte chain. For example, $n_M^c(i_{seg}) = 1.0$ implies that the segment i_{seg} is on the average bound to one macroion.

Figures 3(a) and 3(b) show the complexation function for the flexible and the stiff polyelectrolyte, respectively, at all salt concentrations considered. The complexation functions display mirror symmetry with respect to a reflection at $i_{seg} = (N_{seg}+1)/2$, and as expected the two halves of the chain experience on the average the same environment.

The highest n_M^c value is achieved at $c_{salt} = 0$, and the complexation function decreases monotonically as c_{salt} is increased. The middle segments of the polyelectrolytes (loosely referred to as the binding region) have the highest probability to complex to a macroion.

At low c_{salt}, the complexation functions display peaks near the ends of the chains, the peaks being more accentuated for the stiffer chain. The enhanced probability of macroions to be complexed near the ends is most likely due to the repulsive macroion-macroion potential in combination with a nearly linear arrangement of them, giving rise to an outward repulsion in the same spirit as hard spheres near a surface are pushed by neighboring hard spheres toward the surface.

Throughout, the end segments display a lower probability to become complexed with the macroions signalling an appearance of short tails. At low c_{salt}, there is a considerable difference in the magnitude of n_M^c between the central binding region and the end segments, this effect being decreased when c_{salt} is increased, and at high c_{salt} it has nearly vanished. However, the number of segments being affected does not seem to depend strongly on c_{salt}; rather it depends more on the chain flexibility [17].

For the flexible chain, the magnitude of N_M^c is generally larger than that of the stiff one at the same c_{salt}. At low c_{salt}, $n_M^c(i_{seg}) > 1$ appears for the flexible chain indicating that a segment can be near to more than one macroion simultaneously [cf. Fig. 1(a)]. Given the similar number of complexed macroions N_M^c, there are thus a larger number of segments near a macroion in the case of the flexible chain. This is further quantified in Table II, which provides the number of complexed segments near a complexed macroion, n_{seg}, at different c_{salt}. As c_{salt} is increased from 0 to 300 mM, n_{seg} reduces from 7.6 to 5.0 (interpreted as partial unwrapping) for the flexible polyelectrolyte and from 4.2 to 3.8 for the stiffer one. Thus, the reduction of n_M^c as c_{salt} increases is for the flexible chain both an effect of reduced number of complexed macroions (smaller N_M^c) and of reduced number of polyelectrolyte segments near the complexed macroion (smaller n_{seg}).

C. Polyelectrolyte extension

The spatial extensions of the polyelectrolytes have been quantified by calculating their root-mean-square radius of gyration $\langle R_G^2 \rangle^{1/2}$. Figure 4 displays the radius of gyration of the polyelectrolytes as a function of the salt concentration, and the corresponding simulated data for macroion-free solutions are also included. Regarding the flexible polyelectrolyte, in the absence of macroions $\langle R_G^2 \rangle^{1/2}$ decreases as c_{salt} is increased owing to the screening of the intrachain electrostatic repulsion, whereas at $c_{salt} = 0$ the addition of macroions leads to a reduction of the chain extension by $\approx 35\%$. However, most interestingly $\langle R_G^2 \rangle^{1/2}$ remains essentially unaffected upon addition of salt to the polyelectrolyte-macroion solution, indicating that as c_{salt} is increased the enhanced screening by the small ions is matched by a reduced chain contraction due to the macroion release. Finally, Fig. 4 shows that $\langle R_G^2 \rangle^{1/2}$ of the stiff polyelectrolyte is essentially unaffected by both the addition of salt and of oppositely charged macroions.

D. Macroion structure

Figure 5 provides macroion-macroion radial distribution functions $g_{MM}(r)$ for the two different polyelectrolytes at

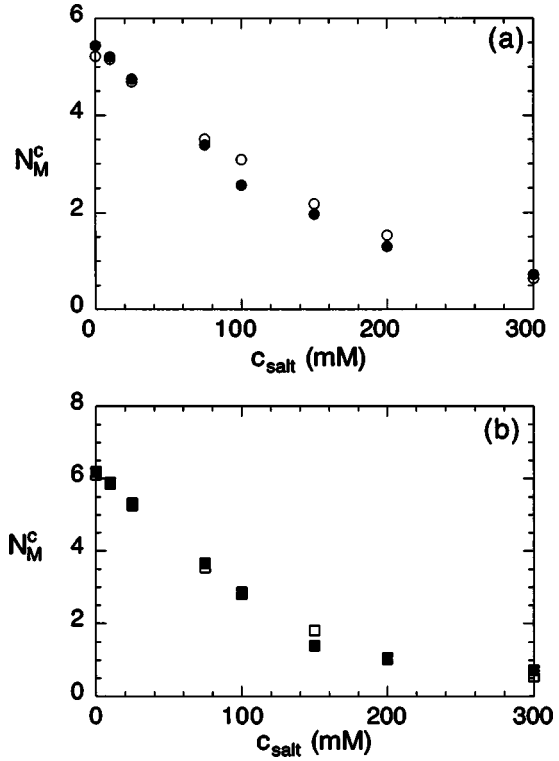

FIG. 6. Number of complexed macroions (N_M^c) vs the salt concentration (c_{salt}) for (a) the flexible and (b) the stiff polyelectrolyte using the primitive model (filled symbols) and the screened Coulomb model (open symbols). Largest estimated uncertainties are $\sigma = 0.1$ for the primitive and 0.05 for the screened Coulomb model.

$c_{\mathrm{salt}}=0$ and 100 mM. The first maximum appears at $r\approx 35$ and 40 Å for the flexible and the stiff polyelectrolyte, respectively, and it arises from pairs of macroions residing in the complex. The shorter macroion-macroion separation for the flexible polyelectrolyte is attributed to the stronger accumulation of polyelectrolyte segments near them (see Table II). The magnitude of the first maximum is reduced upon addition of salt, which is related to the smaller number of macroions in the complex (see Fig. 2). The locations of the maxima are unaffected by the salt concentration, showing that the macroion-macroion separation of nearby macroions in the complex is essentially independent of the salt content.

E. Primitive model versus screened Coulomb model

Figure 6 displays the binding functions of the polyelectrolyte-macroion complexes as a function of the salt concentration using the primitive model (filled symbols) and the screened Coulomb model (open symbols) for the flexible [Fig. 6(a)] and the stiff [Fig. 6(b)] chain. Independent of the chain flexibility, a good agreement between the two models is obtained. Nevertheless, at intermediate c_{salt} the electrostatic screening is somewhat exaggerated by screened Coulomb model, in particular for the flexible polyelectrolyte. Other analyses (data not shown) confirm the similarity of the predictions of the two models.

In a recent contribution, the complexation in a solution of oppositely charged polyelectrolytes was investigated by Monte Carlo simulations using both the primitive model and the screened Coulomb model [23]. The structure of the solution was determined at different ratio of the positively and negatively polyelectrolytes. Also here, the properties of the system as predicted by screened Coulomb model were in near quantitative agreement with those obtained using the primitive model.

F. Counterion release

Previous investigations employing the primitive model have shown that the complexation between polyelectrolytes and oppositely charged macroions is driven both by enthalpic and entropic contributions [29]. It is generally accepted that the latter contribution is dominated by a release of counterions located near the complexing species. In the primitive model with explicit counterions, this release is of course directly observable [16,29]. In the following, we will examine how the Debye-Hückel theory accounts for this release thermodynamically.

Generally, a microscopic quantity becomes temperature dependent as classical degrees of freedom are integrated out. When considering the potential energy, it hence becomes a free energy. A separation of the free energy A into enthalpic and entropic terms can be achieved by using the standard thermodynamic relations $U=\partial(\beta A)/\partial\beta$ and $TS=\beta(\partial A/\partial\beta)$ with $\beta\equiv 1/(kT)$.

Within the framework of the Debye-Hückel theory, the screened Coulomb potential between two charge species is averaged over the positions of the small ions and is given by

$$U^{\mathrm{eff}}(r)=\frac{Z_1Z_2e^2}{4\pi\varepsilon_0\varepsilon_r}\frac{\exp(-\kappa r)}{r}. \tag{7}$$

For simplcity, we have here omitted the effects of the hard spheres [cf. Eq. (4)]. The identification $A=U^{\mathrm{eff}}$ and the fact that $\kappa\sim\beta^{1/2}$ lead to the separation $U^{\mathrm{eff}}=U-TS$ with

$$\frac{U^{\mathrm{eff}}(r)}{Z_1Z_2l_B\kappa kT}=\frac{\exp(-\kappa r)}{\kappa r},$$

$$\frac{U(r)}{Z_1Z_2l_B\kappa kT}=\left(1-\frac{\kappa r}{2}\right)\frac{\exp(-\kappa r)}{\kappa r}, \tag{8}$$

$$\frac{TS(r)}{Z_1Z_2l_B\kappa kT}=\tfrac{1}{2}\exp(\kappa r),$$

where $l_B\equiv e^2/(4\pi\varepsilon_0\varepsilon_r kT)$ denoting the Bjerrum length has been introduced. Thus, when two species of opposite charge, i.e., $Z_1Z_2<0$, are approached, the entropy increases signalling a counterion release.

A subsequent and analogous separation of U given by Eq. (8) into enthalpic and entropic terms can be performed by noticing that also ε_r is temperature dependent. Such a separation will provide information on the entropy of the solvent associated with the orientational ordering of the solvent molecules originating from the electrostatic fields of the charged colloidal species [30].

IV. CONCLUSIONS

On the basis of Monte Carlo simulations, we have investigated the complexation between one polyelectrolyte and oppositely charged macroions in a solution with excess of macroions at different content of simple salt. In absence of salt, an overcharged complex is formed, and at increasing salt content a successive release of macroions appears. This is in line with observations that phase separated solutions of oppositely charged macromolecules tend to mix as salt is added. The number of polyelectrolyte segments near a charged macroion reduces substantially for the flexible chain, whereas remains nearly constant but at a lower value for the stiffer one at increasing salt content.

For the present system, the simplified screened Coulomb model of the extended Debye-Hückel type displayed results in good agreement with the primitive model, suggesting that the salt behavior of such systems can be examined by such a salt-averaged potential. Nevertheless, the primitive model is still a simplistic model. Its foundation has to be assessed, in particular at high salt content where some of its approximations become questionable, for further advances in the understanding of charged colloidal solutions.

ACKNOWLEDGMENTS

Valuable discussions with Håkan Wennerström are gratefully acknowledged. The work was supported by grants from the Foundation of Strategic Research (SSF), through National Graduate School in Scientific Computing (NGSSC), the Swedish Research Council for Engineering Science (TFR), the Swedish National Research Council (NFR), and by computing resources by the Swedish Council for Planning and Coordination of Research (FRN) and the National Supercomputer Center (NSC) Linköping University.

[1] J.-L. Barrat and J.-F. Joanny, Adv. Chem. Phys. **1996**, 66 (1996).
[2] I. D. Robb, in *Anionic Surfactants—Physical Chemistry of Surfactant Action*, edited by E. Lucassen-Reynders (Dekker, New York, 1981), Vol. 11.
[3] G. B. Sukhorukov, E. Donath, S. Davis, H. Lichtenfield, F. Caruso, V. I. Popov, and H. Möhwald, Polym. Adv. Technol. **9**, 759 (1998).
[4] A. Tsuboi, T. Izumi, M. Hirata, J. Xia, P. L. Dubin, and E. Kokufuta, Langmuir **12**, 6295 (1996).
[5] J. Xia and P. L. Dubin, in *Macromolecular Complexes in Chemistry and Biology*, edited by P. Dubin, J. Bock, R. Davis, D. N. Schulz, and C. Thies (Springer-Verlag, Berlin, 1994).
[6] H. G. Bungenberg de Jong, in *Colloid Science*, edited by H. R. Kruyt (Elsevier, Amsterdam, 1949), Vol. 2.
[7] J. E. Scott, Methods Biochem. Anal **8**, 145 (1960).
[8] K. Thalberg, B. Lindman, and G. Karlström, J. Phys. Chem. **95**, 6004 (1991).
[9] Y. Wang, K. Kimura, Q. Huang, P. L. Dubin, and W. Jaeger, Macromolecules **32**, 7128 (1999).
[10] F. Guillemet and L. Piculell, J. Phys. Chem. **99**, 9201 (1995).
[11] T. D. Yager, C. T. McMurray, and K. E. van Holde, Biochemistry **28**, 2271 (1989).
[12] R. R. Netz and J.-F. Joanny, Macromolecules **32**, 9026 (1999).
[13] K.-K. Kunze and R. R. Netz, Phys. Rev. Lett. **85**, 4389 (2000).
[14] T. T. Nguyen and B. I. Shklovskii, J. Chem. Phys. **115**, 7298 (2001).
[15] H. Schiessel, R. Bruinsma, and W. M. Gelbart, J. Chem. Phys. **115**, 7245 (2001).
[16] M. Jonsson and P. Linse, J. Chem. Phys. **115**, 3406 (2001).
[17] M. Jonsson and P. Linse, J. Chem. Phys. **115**, 10975 (2001).
[18] M. J. Stevens and K. Kremer, J. Phys. II **6**, 1607 (1996).
[19] J. P. Valleau, J. Chem. Phys. **129**, 163 (1989).
[20] G. A. Christos and S. L. Camie, J. Chem. Phys. **92**, 7661 (1990).
[21] C. E. Woodward and B. Jönsson, J. Chem. Phys. **155**, 207 (1991).
[22] M. Ullner and C. E. Woodward, Macromolecules **33**, 7144 (2000).
[23] Y. Hayashi, M. Ullner, and P. Linse, J. Chem. Phys. **116**, 6836 (2002).
[24] M. Boström, D. R. M. Williams, and B. W. Ninham, Langmuir **17**, 4475 (2001).
[25] M. Boström, D. R. M. Williams, and B. W. Ninham, Phys. Rev. Lett. **87**, 168103 (2001).
[26] A. Akinchina and P. Linse, Macromolecules **35**, 5183 (2002).
[27] M. P. Allen and D. J. Tildesley, *Computer Simulations of Liquids* (Oxford, New York, 1987).
[28] P. Linse, computer code MOLSIM (Lund University, Sweden, 1999).
[29] T. Wallin and P. Linse, Langmuir **12**, 305 (1996).
[30] D. F. Evans and H. Wennerström, *The Colloidal Domain where Physics, Chemistry, Biology, and Technology meet* (VCH, New York, 1994).